Published in "Journal of Neurophysiology 103: 371-381, 2010"
which should be cited to refer to this work.

Compensatory Regulation of $Ca_v2.1$ Ca^{2+} Channels in Cerebellar Purkinje Neurons Lacking Parvalbumin and Calbindin D-28k

Lisa Kreiner,[1] Carl J. Christel,[3] Morris Benveniste,[2] Beat Schwaller,[4] and Amy Lee[1,3]

[1]*Department of Pharmacology, Emory University;* [2]*Neuroscience Institute, Morehouse School of Medicine, Atlanta, Georgia;* [3]*Department of Molecular Physiology and Biophysics, University of Iowa, Iowa City, Iowa; and* [4]*Department of Medicine, Unit of Anatomy, University of Fribourg, Fribourg, Switzerland*

Kreiner L, Christel CJ, Benveniste M, Schwaller B, Lee A. Compensatory regulation of $Ca_v2.1$ Ca^{2+} channels in cerebellar Purkinje neurons lacking parvalbumin and calbindin D-28k. *J Neurophysiol* 103: 371–381, 2010. First published November 11, 2009; doi:10.1152/jn.00635.2009. $Ca_v2.1$ channels regulate Ca^{2+} signaling and excitability of cerebellar Purkinje neurons. These channels undergo a dual feedback regulation by incoming Ca^{2+} ions, Ca^{2+}-dependent facilitation and inactivation. Endogenous Ca^{2+}-buffering proteins, such as parvalbumin (PV) and calbindin D-28k (CB), are highly expressed in Purkinje neurons and therefore may influence $Ca_v2.1$ regulation by Ca^{2+}. To test this, we compared $Ca_v2.1$ properties in dissociated Purkinje neurons from wild-type (WT) mice and those lacking both PV and CB (PV/$CB^{-/-}$). Unexpectedly, P-type currents in WT and PV/$CB^{-/-}$ neurons differed in a way that was inconsistent with a role of PV and CB in acute modulation of Ca^{2+} feedback to $Ca_v2.1$. $Ca_v2.1$ currents in PV/$CB^{-/-}$ neurons exhibited increased voltage-dependent inactivation, which could be traced to decreased expression of the auxiliary $Ca_v\beta_{2a}$ subunit compared with WT neurons. Although $Ca_v2.1$ channels are required for normal pacemaking of Purkinje neurons, spontaneous action potentials were not different in WT and PV/$CB^{-/-}$ neurons. Increased inactivation due to molecular switching of $Ca_v2.1$ β-subunits may preserve normal activity-dependent Ca^{2+} signals in the absence of Ca^{2+}-buffering proteins in PV/$CB^{-/-}$ Purkinje neurons.

INTRODUCTION

In cerebellar Purkinje neurons, voltage-gated $Ca_v2.1$ channels conduct P-type Ca^{2+} currents that trigger dendritic Ca^{2+} spikes (Llinás and Sugimori 1980a,b; Tank et al. 1988) and regulate repetitive firing (Walter et al. 2006; Womack and Khodakhah 2004). $Ca_v2.1$ is concentrated in the soma and dendrites of Purkinje neurons (Westenbroek et al. 1995) and mediates >90% of the whole cell voltage-gated Ca^{2+} current (Jun et al. 1999; McDonough et al. 1997; Mintz et al. 1992). Mouse mutations that inhibit P-type current density inhibit the frequency and precision of spontaneous firing (Donato et al. 2006; Walter et al. 2006) and increase intrinsic excitability in Purkinje neurons (Ovsepian and Friel 2008). Given the importance of Purkinje neurons in the control of motor function (Ito 1984), these cellular defects invariably cause ataxia (Sidman 1965; Snell 1955).

Like other Ca_v channels, $Ca_v2.1$ is directly modulated by Ca^{2+} ions that permeate the channel. During repetitive depolarizations, $Ca_v2.1$ channels undergo Ca^{2+}-dependent facilitation followed by inactivation (Chaudhuri et al. 2005; DeMaria et al. 2001; Lee et al. 2000). These effects rely on Ca^{2+} binding to calmodulin, which interacts directly with the pore-forming $Ca_v2.1$ subunit ($\alpha_1 2.1$), and are absent for $Ca_v2.1$ Ba^{2+} currents (DeMaria et al. 2001; Lee et al. 1999). Ca^{2+}-dependent inactivation, but not facilitation, is blunted by intracellular dialysis with Ca^{2+} chelators such as ethylene glycol tetraacetic acid (EGTA) (Lee et al. 2000). These findings suggest that Ca^{2+}-dependent facilitation depends on rapid, local Ca^{2+} signals through individual channels, whereas Ca^{2+}-dependent inactivation relies on slower, global Ca^{2+} elevations supported by multiple neighboring channels (DeMaria et al. 2001; Liang et al. 2003; Soong et al. 2002).

The sensitivity of Ca^{2+}-dependent inactivation to Ca^{2+} chelators has important implications for $Ca_v2.1$ channels in Purkinje neurons. These neurons have high endogenous Ca^{2+}-buffering capacity due in part to the Ca^{2+}-binding proteins parvalbumin (PV) and calbindin D-28k (CB) (Celio 1990; Fierro et al. 1998). By chelating free Ca^{2+}, the two proteins and, more importantly, CB directly modulate the kinetics of synaptically evoked Ca^{2+} transients in Purkinje cell dendrites (Schmidt et al. 2003, 2007). PV and CB can also indirectly shape Ca^{2+} signals by controlling Ca^{2+} ions that are available for feedback regulation of $Ca_v2.1$. Like EGTA, coexpression of PV or CB with $Ca_v2.1$ in HEK293T cells can suppress Ca^{2+}-dependent inactivation without affecting facilitation (Kreiner and Lee 2006). Therefore PV and CB may alter Ca^{2+} feedback regulation of $Ca_v2.1$ in Purkinje neurons.

To test this, we compared P-type currents in dissociated Purkinje neurons from wild-type (WT) mice and those lacking expression of PV and CB (PV/$CB^{-/-}$). Voltage-dependent inactivation but not Ca^{2+}-dependent inactivation was greater in PV/$CB^{-/-}$ than in WT neurons, which could be explained by down-regulation of the auxiliary $Ca_v\beta_{2a}$ subunit. Our findings suggest a new role for Ca^{2+}-binding proteins in maintaining $Ca_v2.1$ function and also suggest a compensatory mechanism by which Ca^{2+} homeostasis may be achieved in the absence PV and CB.

METHODS

Purkinje cell dissociation

Animal procedures complied with National Institutes of Health guidelines and were conducted under a protocol approved by Emory Institutional Animal Care and Use Committee. PV and CB double-knockout mice (PV/$CB^{-/-}$) were characterized previously (Vecellio et al. 2000) and maintained on the Sv129×C57/BL6 strain, which served as the WT group. Postnatal day 14 (P14) to P21 mice were anesthetized with isoflurane and decapitated. Sagittal cerebellar slices

Address for reprint requests and other correspondence: A. Lee, Department of Molecular Physiology and Biophysics, University of Iowa, 5-611 Bowen Science Bldg., 51 Newton Road, Iowa City, IA 52242 (E-mail: amy-lee@uiowa.edu).

(400 μm) were cut on a vibratome and held in Tyrode solution (in mM: 150 NaCl, 4 KCl, 2 $CaCl_2$, 2 $MgCl_2$, 10 HEPES, 10 glucose, adjusted to pH 7.4 with NaOH) at 34°C for 30 min before allowing them to cool to room temperature. Immediately prior to recording, slices were incubated for 10 min in papain (1 mg/ml; Worthington, Lakewood, NJ) dissolved in dissociation solution (in mM: 82 Na_2SO_4, 30 K_2SO_4, 5 $MgCl_2$, 10 HEPES, and 10 glucose, adjusted to pH 7.4 with NaOH). Slices were then washed in Tyrode solution, placed in a fresh tube containing 1 ml Tyrode solution, and dissociated by gentle trituration through a series of fire-polished pipettes. Supernatant containing dissociated cells was placed on poly-L-lysine–coated coverslips for electrophysiological recording. Dissociated Purkinje neurons were readily distinguished from surrounding cells by their large, pear-shaped soma and dendritic stump.

HEK293T cell culture and transfection

HEK293T cells were maintained in Dulbecco's modified Eagle's medium supplemented with 10% fetal bovine serum at 37°C under 5% CO_2. Cells plated in 35-mm tissue-culture dishes were grown to 65–80% confluency and transfected with GenePORTER transfection reagent (Gene Therapy Systems, San Diego, CA), according to the manufacturer's protocol, with a 1:1 molar ratio of cDNAs for Ca^{2+} channel subunits: rat $\alpha_1$2.1 (rbA isoform; Stea et al. 1994), β_{2a} (Perez-Reyes et al. 1992) or β_4 (Castellano et al. 1993), $\alpha_2\delta$ (Starr et al. 1991; total 5 μg), and 0.7 μg of a CD8 expression plasmid. At least 48 h after transfection, cells were incubated with CD8 antibody-coated microspheres (Dynal, Oslo, Norway) for identification of transfected cells for electrophysiological recording.

Electrophysiological recordings

Ca^{2+} or Ba^{2+} currents were recorded in transfected HEK293T cells and Purkinje neurons in whole cell patch-clamp configuration at room temperature. Extracellular recording solutions for HEK293T cells contained (in mM): 150 Tris, 1 $MgCl_2$, and 10 $CaCl_2$ or 10 $BaCl_2$. Intracellular recording solutions contained (in mM): 130 *N*-methyl-D-glucamine, 60 HEPES, 1 $MgCl_2$, 2 Mg-ATP, and 0.5 EGTA. The pH of extracellular and intracellular recording solutions was adjusted to 7.3 with methanesulfonic acid. For voltage-clamp recordings of Purkinje neurons, extracellular solutions were optimized for stable whole cell recordings of Ca_v2.1 currents and contained (in mM): 155 tetraethylammonium chloride (TEA), 10 HEPES, 1 EGTA, and 10 $CaCl_2$ or 2 or 10 $BaCl_2$, adjusted to pH 7.4 with TEA-OH. Prior to recording, tetrodotoxin (TTX, 1 μM) and nimodipine (5 μM) were included in the extracellular recording solution to block Na^+ and L-type Ca^{2+} currents, respectively. Intracellular solutions contained (in mM): 140 Cs methanesulfonate, 4 $MgCl_2$, 0.5 EGTA, 9 HEPES, 14 creatine phosphate (Tris salt), 4 Mg adenosine 5′-triphosphate (ATP), and 0.3 Tris-GTP, adjusted to pH 7.4 with CsOH. For current-clamp recordings, Tyrode solution was used for the extracellular solution and the intracellular recording solution contained (in mM): 140 K-methyl sulfate, 10 KCl, 5 NaCl, 0.01 EGTA, 10 HEPES, and 2 Mg-ATP, adjusted to pH 7.4 with KOH. Electrode resistances in the recording solutions were typically 1–2 MΩ for Purkinje neurons and 2–4 MΩ for HEK293T cells. Reagents used for electrophysiological recordings were obtained from Sigma–Aldrich (St. Louis, MO).

Currents were recorded with an EPC-9 patch-clamp amplifier driven by PULSE software (HEKA Electronics, Lambrecht/Pfalz, Germany). Leak and capacitive transients were subtracted using a P4 protocol. Action potential (AP) waveforms were constructed by averaging traces corresponding to spontaneous APs recorded in current clamp from dissociated WT Purkinje neurons. The AP waveform was applied from a holding potential of −60 mV and had a half-width of 0.75 ms and peak amplitude of +25 mV for Purkinje neuron recordings. For transfected HEK293T cell recordings, the waveform was scaled to peak at +55 mV. Data were analyzed using routines written in IGOR Pro software (WaveMetrics, Lake Oswego, OR). Averaged data represent the means ± SE. Statistical differences between groups were determined by Student's *t*-test. Current–voltage (*I–V*) curves were fit with the function: $g(V - E)/\{1 + \exp[(V - V_{1/2})/k] + b\}$, where g is the maximum conductance, V is the test potential, E is the apparent reversal potential, $V_{1/2}$ is the potential of half-activation, k is the slope factor, and b is the baseline. Significant differences between *I–V* curve values were determined with two-way repeated-measures ANOVA.

PCR analysis

For endpoint polymerase chain reaction (PCR), total RNA was isolated from cerebellar tissue using Trizol reagent (Invitrogen, Carlsbad, CA) according to the manufacturer's protocol. Reverse transcription was performed on 2 μg RNA using random hexamers and Superscript II reverse transcriptase (Invitrogen) at 42°C for 50 min. For isolated Purkinje neurons, the entire neuron was harvested by suction into an electrode containing intracellular recording solution. The tip of the pipette was then pressurized and broken to expel the cell into a tube containing reverse transcription reagents. Following overnight incubation at 40°C, the samples were used immediately or stored at −80°C. PCR reactions were performed with GoTaq Green Master Mix (Promega, Madison, WI) or *Taq* DNA polymerase (New England BioLabs, Ipswich, MA) and a Mastercycler (Eppendorf, Westbury, NY). PCR products were visualized by electrophoresis on 1–2% agarose gels prestained with ethidium bromide.

For quantitative PCR, pools of 5–10 Purkinje neurons were isolated for reverse transcription as described earlier. Oligonucleotide primers were designed to amplify approximately 100 basepair mouse sequences for $Ca_v\beta_{2a}$ and glyceraldehyde-3-phosphate dehydrogenase (GAPDH). Amplification of a single band was confirmed initially by endpoint PCR and gel electrophoresis. Quantitative PCR was performed on reverse transcription (RT) reactions (2 μl) according to manufacturer's protocols with the DyNAmo HS SYBR Green qPCR kit (Finnzymes, Woburn, MA) and iCycler (Bio-Rad, Hercules, CA). Samples were run in duplicate for 40 cycles [95°C for 15 min (hot start), 94°C for 20 s, 60°C for 30 s, 72°C for 30 s]. Experiments were repeated at least three times using RNA collected from Purkinje neurons from different mice. Melt curve analysis revealed a single peak in SYBR green fluorescence, confirming amplification of a single product for each primer set. Efficiency of amplification was roughly 100% for each primer set and measured as $[(10^{-1/k} - 1) \times 100]$, where k is the slope of the relationship between cycle threshold [C(t)] and dilution of the RT reaction. Relative change in WT compared with PV/$CB^{-/-}$ neurons was determined by the comparative $C(t)[2^{-\Delta\Delta C(t)}]$ method (Livak and Schmittgen 2001), in which GAPDH was used as the internal control gene. For WT and PV/$CB^{-/-}$ neurons, ΔC(t) was determined as the difference in C(t) for the target ($Ca_v\beta_{2a}$) and C(t) for GAPDH. Percentage WT expression was then determined as: {[ΔC(t) for PV/$CB^{-/-}$] − [ΔC(t) for WT]} × 100%. Primer sequences are listed in Supplemental Table S1.[1]

RESULTS

Characterization of Ca^{2+}-dependent inactivation and facilitation of P-type currents in Purkinje neurons

To allow for comparisons of neuronal P-type currents with Ca_v2.1 currents in transfected cells, recordings were made in whole cell patch configuration. Although this approach could cause dialysis of intracellular components, such as PV and CB, we did not observe significant differences in P-type current properties ≤20 min after membrane patch rupture. However,

[1] The online version of this article contains supplemental data.

voltage protocols were initiated at the same time and run in the same order to minimize variability between cells. Although the absence of exogenous Ca^{2+} chelators in internal recording solutions might allow for maximal resolution of the effects of PV and CB, this approach did not allow stable whole cell recordings. However, the amount of EGTA in the intracellular recording solution was limited to 0.5 mM, which is permissive for Ca^{2+}-dependent inactivation of $Ca_v2.1$ in transfected cells (DeMaria et al. 2001; Lee et al. 1999, 2000).

For our studies, we used Purkinje neurons from mice that were 14–21 days old. This age range was chosen as a compromise between the ability to obtain stable Ca^{2+} current recordings in young neurons and previous findings that mature expression levels of PV and CB are reached near P20 (Schwaller et al. 2002). Since Ca^{2+}-dependent modulation of $Ca_v2.1$ has not been reported in mouse Purkinje neurons at this developmental stage, we first undertook a basic characterization of this process. To isolate P-type currents, whole cell patch-clamp recordings were conducted with extracellular Ca^{2+} (10 mM) and blockers of voltage-gated Na^+ and K^+ channels. Depolarizing steps were made from a holding voltage of −60 mV to minimize contribution of low-voltage–activated T-type currents in these cells (Raman and Bean 1999). Under these conditions, we observed large inward currents that did not inactivate significantly within the 50-ms test pulse. The currents were blocked about 80–90% on extracellular perfusion of the selective $Ca_v2.1$ blocker, ω-agatoxin type IVA (500 nM, Fig. 1*A*). These properties were consistent with the P-type current in rat and mouse Purkinje neurons (Mintz et al. 1992; Raman and Bean 1999; Richards et al. 2007; Usowicz et al. 1992), which is mediated by $Ca_v2.1$ (Jun et al. 1999).

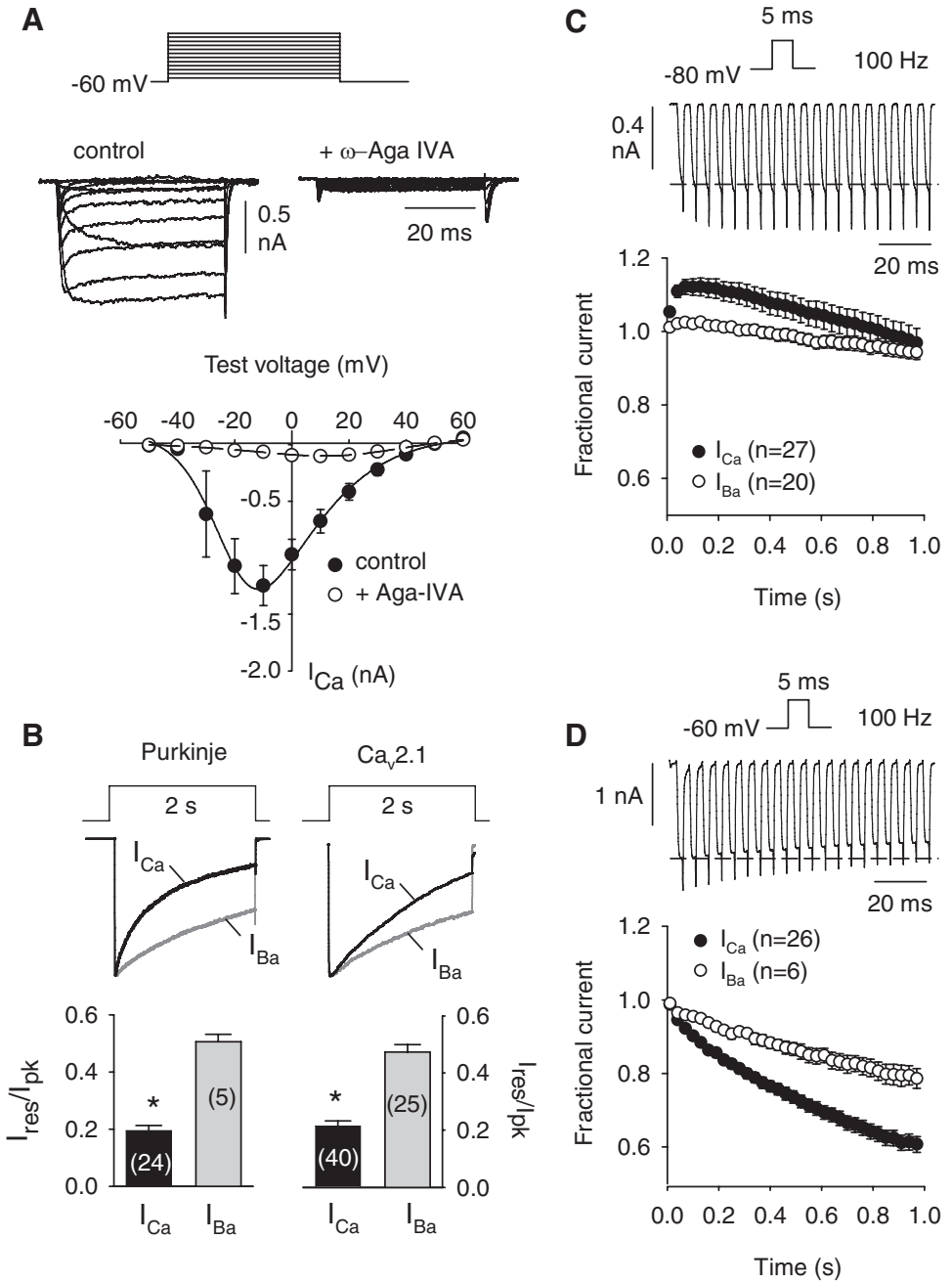

FIG. 1. Ca^{2+}-dependent inactivation of P-type currents in mouse cerebellar Purkinje neurons. *A*: current–voltage (*I–V*) relationships for a Ca^{2+} current (I_{Ca}) evoked by 50-ms steps from −60 mV to various voltages. Shown are representative current traces and voltage protocol (*top*) and *I–V* relationship (*bottom*) in cells before (control, filled circles) and after (+Aga-IVA, open circles) extracellular perfusion with ω-agatoxin-IVA (500 nM). Points represent means ± SE (n = 10). *B*: inactivation of P-type currents in Purkinje neurons and $Ca_v2.1$ ($\alpha_1 2.1$, β_{2a}, $\alpha_2\delta$) in transfected HEK293T cells. In Purkinje neurons, I_{Ca} and Ba^{2+} current (I_{Ba}) were evoked by 2-s pulses from −60 to −10 or −20 mV, respectively, and were evoked in transfected HEK293T cells by 2-s pulses from −80 to +10 or 0 mV, respectively. The −10-mV difference in test pulse used for I_{Ba} accounts for the shift in activation voltage when using Ba^{2+} as the charge carrier. Voltage protocol and current traces for I_{Ca} (black) and I_{Ba} (gray) are shown (*top*). I_{res}/I_{pk} (current amplitude at end of 2-s pulse normalized to peak current amplitude) is plotted below for Purkinje neurons (*left*) and transfected HEK293T cells (*right*). Parentheses indicate numbers of cells. *$P < 0.01$ by *t*-test. *C*: Ca^{2+}-dependent facilitation during repetitive depolarizations in $Ca_v2.1$-transfected HEK293T cells. I_{Ca} and I_{Ba} were recorded during 5-ms steps from −80 to +10 mV (I_{Ca}) or 0 mV (I_{Ba}) delivered at 100 Hz. Fractional current represents test current amplitude normalized to the first in the train and is plotted against time. Every third data point is plotted. *D*: same as in *C* except that pulses were from −60 to 0 mV (I_{Ca}) or −10 mV (I_{Ba}) and applied to Purkinje neurons. In *C* and *D*, representative I_{Ca} and voltage protocols are shown above averaged data. Dashed line represents initial current amplitude.

We next compared inactivation of currents evoked by 2-s-step depolarizations using Ca^{2+} or Ba^{2+} as the permeant ion (Fig. 1*B*). Inactivation was measured as the current amplitude at the end of the test pulse normalized to the peak current amplitude (I_{res}/I_{pk}). With this protocol, Ca^{2+}-dependent inactivation causes stronger inactivation (smaller I_{res}/I_{pk}) for Ca^{2+} currents (I_{Ca}) than for Ba^{2+} currents (I_{Ba}). By convention, inactivation of I_{Ba} is considered as proceeding by a purely voltage-dependent mechanism. As shown in Fig. 1*B*, P-type currents exhibited significant Ca^{2+}-dependent inactivation similar to that of HEK293T cells transfected with cDNAs for $Ca_v2.1$ subunits ($\alpha_1 2.1$, β_{2a}, $\alpha_2\delta$).

In response to a train of 5-ms-step depolarizations, I_{Ca} in $Ca_v2.1$-transfected cells initially increases roughly 10–15% (Fig. 1*C*). This effect is not seen for I_{Ba} and represents Ca^{2+}-dependent facilitation mediated by calmodulin (Lee et al. 2000). The same voltage protocol applied to mouse Purkinje neurons did not produce facilitation but only inactivation of I_{Ca} (Fig. 1*D*). Although the amplitude of facilitated I_{Ca} in $Ca_v2.1$-transfected cells declined to values approximating the initial (nonfacilitated) test current (Fig. 1*C*), I_{Ca} in Purkinje neurons inactivated roughly 60% by the end of the train (Fig. 1*D*). I_{Ba} also inactivated significantly more in Purkinje neurons than in $Ca_v2.1$-transfected cells during this protocol (Fig. 1, *C* and *D*), suggesting greater voltage-dependent inactivation in Purkinje neurons than that in transfected cells. Mechanistically, this could result from slower recovery from, or faster onset of, inactivation, which would increase the accumulation of inactivated channels during trains of depolarizations. Consistent with the latter possibility, inactivation of I_{Ca} in Purkinje neurons proceeded at a faster rate ($\tau = 0.77 \pm 0.07$, $n = 24$) than that in transfected cells ($\tau = 1.20 \pm 0.06$, $n = 40$; $P < 0.001$).

Voltage-dependent inactivation of the P-type current might obscure Ca^{2+}-dependent facilitation during repetitive square-pulse stimuli since shorter depolarizations, such as with AP waveforms, have been shown to induce facilitation of P-type Ca^{2+} currents (Chaudhuri et al. 2005, 2007; Richards et al. 2007). Therefore we developed an AP waveform stimulus based on spontaneous APs measured first in current-clamp recordings (Fig. 2*A*). At 200 Hz, AP waveforms consistently produced an initial facilitation of I_{Ca} (~29 ± 4%) in Purkinje neurons, which decayed rapidly during the 1-s stimulus (Fig. 2, *B* and *C*). With the same protocol, I_{Ba} showed little facilitation (~3 ± 2%), which may result from activity-dependent removal of $Ca_v2.1$ channels from G-protein inhibition (Brody et al. 1997; Park and Dunlap 1998). Facilitation of I_{Ca} was about tenfold greater than that for I_{Ba}, consistent with the magnitude of Ca^{2+}-dependent facilitation in $Ca_v2.1$- trans-

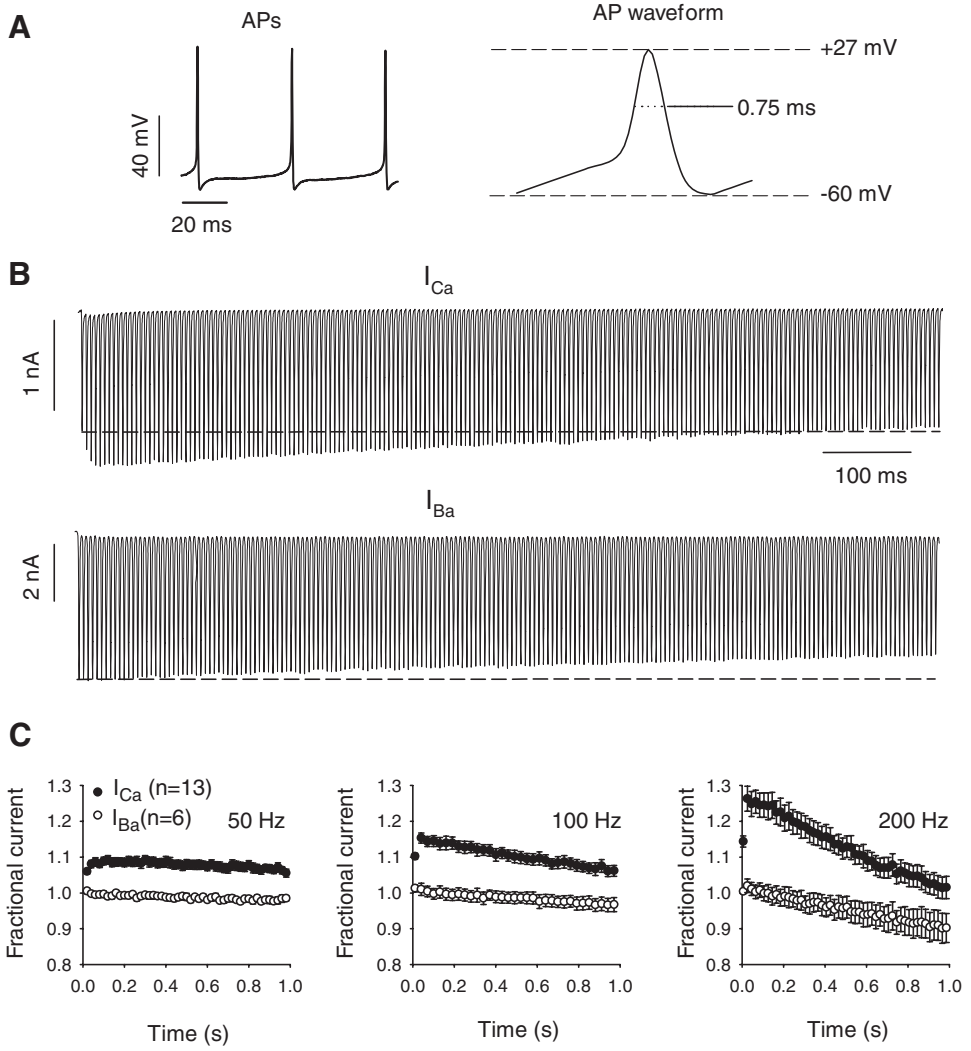

FIG. 2. Ca^{2+}-dependent facilitation in Purkinje neurons during trains of action potential (AP) waveforms. *A*: spontaneous APs recorded in current-clamp (*left*) were used to construct an average AP waveform (*right*) with amplitude (+27 mV) and half-width (0.75 ms) indicated. *B*: representative I_{Ca} and I_{Ba} evoked by the AP waveform stimulus in *A* delivered at 200 Hz. Dashed line indicates current amplitude of the first pulse. *C*: increased Ca^{2+}-dependent facilitation with higher frequency stimulation. Current responses to AP waveforms were measured at 50, 100, and 200 Hz. Fractional current represents test current amplitude normalized to the first in the train and plotted against time. For 100- and 200-Hz data, every third and fourth data point is plotted, respectively.

fected cells (Kreiner and Lee 2006; Lee et al. 2000). Facilitation of I_{Ca} was significantly greater with higher frequency stimulation (29 ± 4% for 200 Hz, 17 ± 2% for 100 Hz, and 11 ± 1% for 50 Hz; $P < 0.001$), which was not observed for I_{Ba} (3 ± 2% for 200 Hz, 2 ± 2% for 100 Hz, and 1 ± 1% for 50 Hz, $P = 0.45$; Fig. 2*C*). These results confirm that P-type currents undergo pronounced Ca^{2+}-dependent facilitation in mouse Purkinje neurons, which would be greatest during periods of rapid firing.

We next asked why voltage-dependent inactivation was stronger in Purkinje neurons than that in our $Ca_v2.1$-transfected cells, since this clearly influenced parameters for uncovering Ca^{2+}-dependent facilitation (Fig. 1, *C* and *D*). We focused on the auxiliary $Ca_v\beta_{2a}$ subunit, used in the transfected cell experiments, which is unique among $Ca_v\beta$ subunits in conferring slow voltage-dependent inactivation to $Ca_v2.1$ (De Waard and Campbell 1995; Stea et al. 1994). Of the four $Ca_v\beta$ variants (β_1, β_2, β_3, β_4,) detected in rodent cerebellum, $Ca_v\beta_{2a}$ and $Ca_v\beta_4$ are most highly expressed in Purkinje neurons (Ludwig et al. 1997; Richards et al. 2007). Relative to $Ca_v\beta_{2a}$, $Ca_v\beta_4$ causes $Ca_v2.1$ to undergo greater voltage-dependent inactivation (Bourinet et al. 1999; Sokolov et al. 2000; Stea et al. 1994). Therefore the inactivating profile of P-type currents in mouse Purkinje neurons may result from the combined contribution of $Ca_v\beta_{2a}$ and $Ca_v\beta_4$. To test this, we compared I_{Ca} and I_{Ba} in Purkinje neurons and HEK293T cells transfected with $Ca_v2.1$ channels containing β_{2a} [$Ca_v2.1(\beta_{2a})$] or β_4 [$Ca_v2.1(\beta_4)$] (Fig. 3, *A–C*). In contrast to square-pulse depolarizations, which caused facilitated I_{Ca} to decay within 0.6 s in cells transfected with $Ca_v2.1(\beta_{2a})$ (Fig. 1*C*), AP waveforms produced facilitation of I_{Ca} that remained maximal from about 0.2 to 0.6 s (Fig. 3*B*). Interestingly, maximal facilitation of I_{Ca} for $Ca_v2.1(\beta_4)$ (28 ± 6%) was not different from that of $Ca_v2.1(\beta_{2a})$ (35 ± 5%, $P = 0.42$), but declined rapidly within 0.6 s (Fig. 3*C*). Thus the identity of the $Ca_v\beta$ isoform does not affect the maximal amount of Ca^{2+}-dependent facilitation during AP waveform stimuli, but rather how long Ca^{2+}-dependent facilitation lasts. The decline in the amplitude of the facilitated I_{Ca} in $Ca_v2.1(\beta_4)$-transfected cells was likely due to the onset of voltage-dependent inactivation, which was apparent in comparing the rapid decay of I_{Ba} for $Ca_v2.1(\beta_4)$ with the maintained amplitude of I_{Ba} for $Ca_v2.1(\beta_{2a})$ (Fig. 3, *B* and *C*). With Ca^{2+} or Ba^{2+} as the charge carrier, the neuronal P-type currents evoked by AP waveforms inactivated to a level intermediate to that for $Ca_v2.1(\beta_{2a})$ and $Ca_v2.1(\beta_4)$ (Fig. 3, *D* and *E*). Coexpression of β_{2a} and β_4 in HEK293T cells yielded $Ca_v2.1$ currents that inactivated to an extent similar to that of P-type currents in Purkinje neurons (Fig. 3, *D* and *E*). However, the initial rise time of the facilitated I_{Ca} was considerably faster in Purkinje neurons than in HEK293T cells transfected with any combination of β subunits, perhaps due to the expression of distinct $\alpha_1 2.1$ splice variants in Purkinje neurons (Chaudhuri et al. 2005; Richards et al. 2007). Nevertheless, these findings suggest that voltage-dependent inactivation and, subsequently, the maintenance of Ca^{2+}-dependent facilitation depend on the ratio of $Ca_v\beta_{2a}$ and $Ca_v\beta_4$ subunits in Purkinje neurons.

Comparison of P-type currents in WT and PV/CB$^{-/-}$ neurons

Having established that P-type currents in mouse Purkinje neurons undergo Ca^{2+}-dependent inactivation and facilitation, we next evaluated the role of endogenous Ca^{2+} buffers in Purkinje neurons. Due to their high expression levels in Purkinje neurons, the Ca^{2+}-binding proteins, PV and CB, may

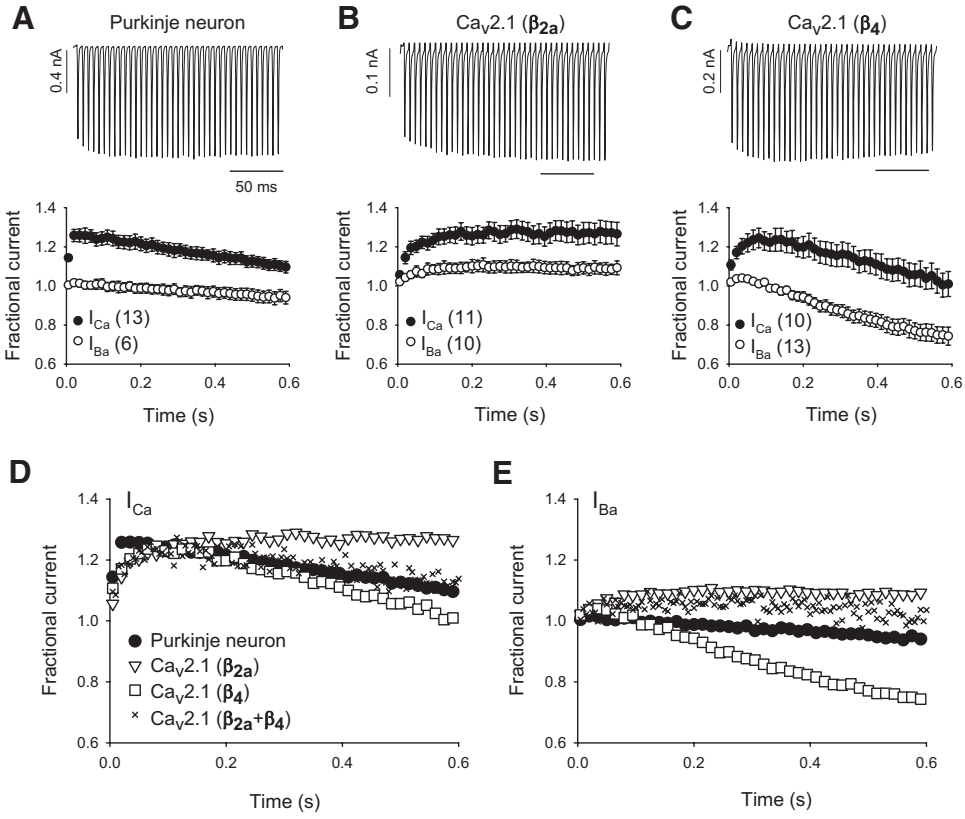

FIG. 3. $Ca_v\beta$ subunits influence the profile of $Ca_v2.1$ currents during AP stimuli. I_{Ca} and I_{Ba} were evoked by AP waveforms at 200 Hz. Representative I_{Ca} (*top*) and fractional current measured as in Fig. 2*C* (*bottom*) in Purkinje neurons (*A*) and HEK293T cells transfected with $\alpha_1 2.1$, $\alpha_2\delta$, and β_{2a} (*B*) or β_4 (*C*). Parentheses indicate numbers of cells. Results in *A–C* and for cells cotransfected with β_{2a} and β_4 for I_{Ca} (*D*) and I_{Ba} (*E*) are superimposed on the same graph for comparison. For clarity, error bars were omitted in *D* and *E* and, for each graph, every third data point is plotted. For HEK293T cells cotransfected with both β_{2a} and β_4, results from exemplar cells are shown.

inhibit Ca^{2+}-dependent inactivation in a manner similar to that of EGTA and BAPTA [1,2-bis(*o*-aminophenoxy)ethane-*N*,*N*,*N*′,*N*′-tetraacetic acid] (Lee et al. 2000). Since Ca^{2+}-dependent facilitation of $Ca_v2.1$ is mediated by local Ca^{2+} signals not affected by EGTA and BAPTA (DeMaria et al. 2001; Lee et al. 2000; Liang et al. 2003), PV and CB should not affect Ca^{2+}-dependent facilitation. If so, then Ca^{2+}-dependent inactivation but not facilitation should be greater in Purkinje neurons lacking PV and CB. To test this, we compared P-type currents in Purkinje neurons isolated from WT and PV/$CB^{-/-}$ mice.

In general, P-type currents in WT and PV/$CB^{-/-}$ neurons showed similar activation properties, although the amplitude of I_{Ca} was generally greater in PV/$CB^{-/-}$ than that in WT neurons (Supplemental Table S2). There were no significant differences in cell capacitance (16.9 ± 0.6 pF for WT vs. 17.6 ± 0.7 pF for PV/$CB^{-/-}$, $P = 0.45$) or the extent of block by ω-agatoxin IVA (90.0 ± 1.6% for WT vs. 84.4 ± 8.3% for PV/$CB^{-/-}$; $P = 0.20$; Fig. 4). These results indicated that genetic deletion of PV and CB did not influence the contribution of $Ca_v2.1$ to the whole cell Ca^{2+} current in Purkinje neurons.

If PV and CB specifically attenuated Ca^{2+}-dependent inactivation, we would expect an increase in inactivation of I_{Ca} in PV/$CB^{-/-}$ compared with that in WT neurons; the decay of I_{Ba} due to voltage-dependent inactivation should not be affected. However, we found that both I_{Ca} and I_{Ba} underwent greater inactivation in PV/$CB^{-/-}$ than that in WT neurons (Fig. 5, *A* and *B*). Since I_{Ca} inactivation contains both Ca^{2+}-dependent and voltage-dependent components, we measured the difference between I_{res}/I_{pk} for I_{Ca} and I_{Ba} to isolate Ca^{2+}-dependent inactivation and found that it was similar in WT and PV/$CB^{-/-}$ neurons (Fig. 5*A*). Together, these results indicate that voltage-dependent inactivation is increased in PV/$CB^{-/-}$ compared with that in WT neurons. Kinetic analyses showed significantly faster rates of inactivation for I_{Ba} in PV/$CB^{-/-}$ ($\tau = 1.05 \pm 0.06$, $n = 12$) than those in WT ($\tau = 1.69 \pm 0.23$, $n = 15$; $P = 0.02$) neurons, although there was no difference in inactivation rate for I_{Ca} ($\tau = 0.77 \pm 0.07$, $n = 24$, for WT vs. $\tau = 0.72 \pm 0.05$, $n = 23$, for PV/$CB^{-/-}$; $P = 0.5$). Stronger voltage-dependent inactivation in PV/$CB^{-/-}$ neurons was particularly apparent at high stimulation frequencies (Fig. 6, *A–D*): P-type currents during 200-Hz AP waveforms decayed to initial levels within 0.4 s in PV/$CB^{-/-}$ neurons, whereas currents in WT neurons remained strongly facilitated (~20%) at this time point (Fig. 6, *C* and *D*).

Because the stronger voltage-dependent inactivation in PV/$CB^{-/-}$ neurons could not be linked directly to the absence of Ca^{2+} buffers, we hypothesized that the differences in P-type currents in WT and PV/$CB^{-/-}$ neurons could have arisen from a compensatory change in $Ca_v2.1$ subunit expression. As alluded to in Fig. 3, a decrease in the ratio of $Ca_v\beta_{2a}$ and $Ca_v\beta_4$ could boost the number of $Ca_v2.1$ channels undergoing strong voltage-dependent inactivation. We tested this possibility by PCR of isolated Purkinje neurons with primers specific for the different $Ca_v\beta$ subunits (Fig. 7, *A–D*). Because dissociated preparations of Purkinje neurons also contain a vast number of

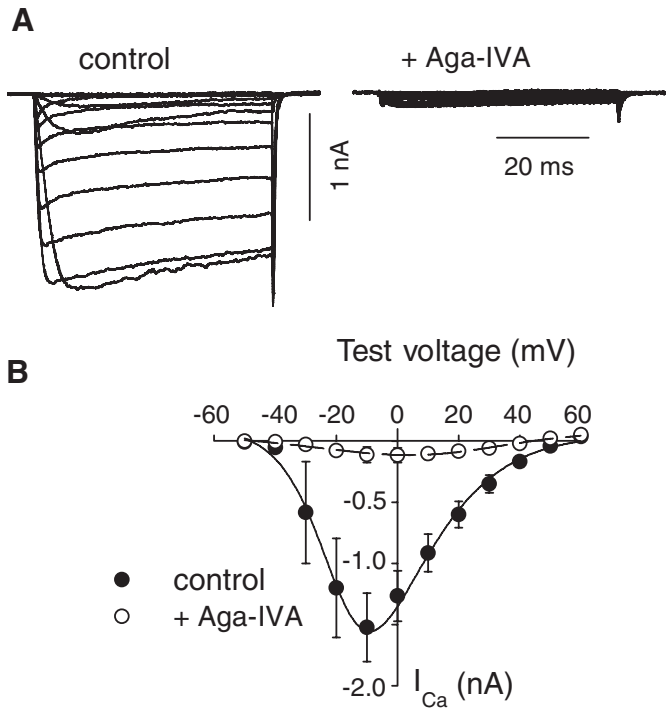

FIG. 4. Characterization of P-type currents in PV/$CB^{-/-}$ Purkinje neurons. *A*: representative current I_{Ca} (*A*) and *I–V* relationship (*B*) in cells before (filled circles) and after (open circles) exposure to ω-agatoxin IVA (500 nM). Points represent means ± SE ($n = 12$). CB, calbindin D-28k; PV, parvalbumin.

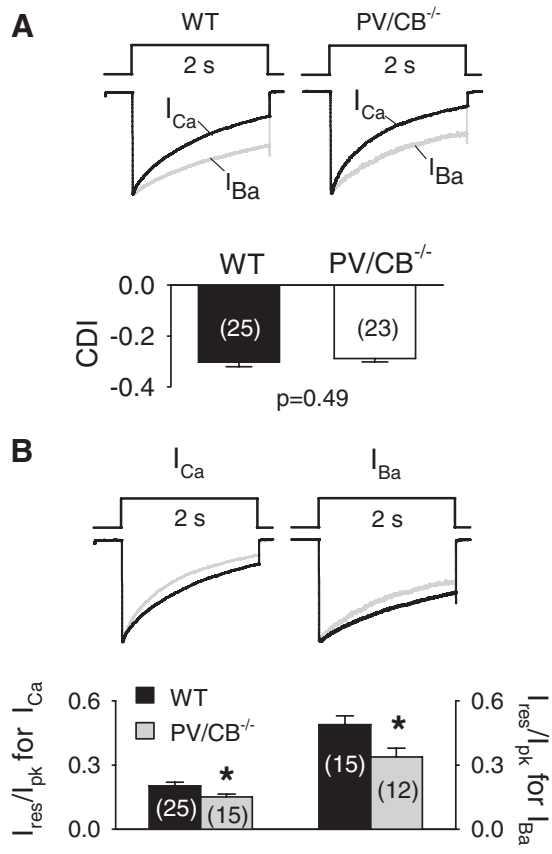

FIG. 5. Increased voltage- but not Ca^{2+}-dependent inactivation (CDI) of $Ca_v2.1$ currents in PV/$CB^{-/-}$ Purkinje neurons. *A*: I_{Ca} and I_{Ba} were evoked by 2-s pulses from −60 to 0 mV (I_{Ca}) or −10 mV (I_{Ba}) in wild-type (WT) and PV/$CB^{-/-}$ neurons. CDI represents the difference in I_{res}/I_{pk} for I_{Ca} and I_{Ba} in WT and PV/$CB^{-/-}$ neurons. *B*: comparison of I_{res}/I_{pk} for I_{Ca} and I_{Ba} (measured with 2 mM extracellular Ba^{2+}) in WT (black traces) and PV/$CB^{-/-}$ neurons (gray traces). *$P < 0.05$ by *t*-test. Parentheses indicate numbers of cells.

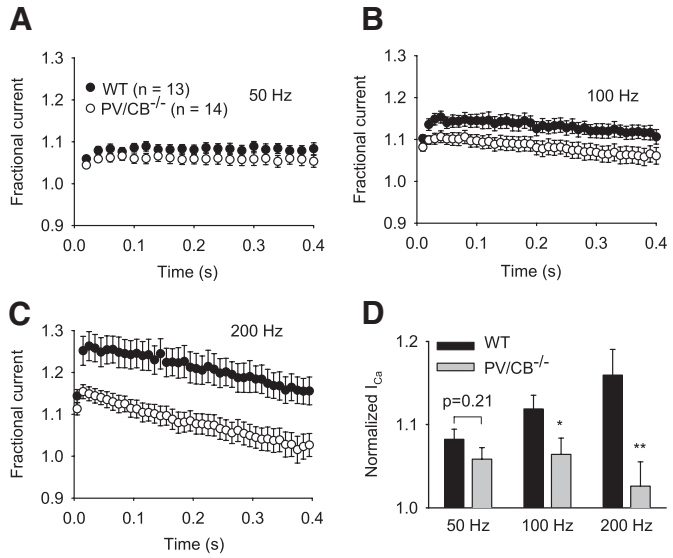

FIG. 6. Increased inactivation of P-type currents during high-frequency stimulation in PV/CB$^{-/-}$ Purkinje neurons. I_{Ca} was evoked by AP waveform stimuli given at 50 (*A*), 100 (*B*), or 200 Hz (*C*) in WT (filled circles) and PV/CB$^{-/-}$ (open circles) Purkinje neurons. Every other point is plotted for 200-Hz data. *D*: normalized I_{Ca} represents the grand average of current amplitude for the last 10 pulses (±SE) plotted against stimulation frequency for WT and PV/CB$^{-/-}$ neurons. $^{**}P < 0.01$; $^{*}P < 0.05$ compared with WT by *t*-test.

other cell types, mainly granule cells, we performed control experiments to ensure that we were isolating nucleic acids mainly from Purkinje neurons. In these experiments, calbindin D-28k mRNA (gene symbol: *Calb1*) was amplified from cerebellum and Purkinje neurons from WT mice but, as expected, not from PV/CB$^{-/-}$ neurons (Fig. 7*A*). In the cerebellum, calretinin (gene symbol: *Calb2*) is not expressed in Purkinje neurons but in unipolar brush cells, Lugaro cells, and predominantly in granule cells (Schwaller et al. 2002). As expected, calretinin mRNA was amplified only from total cerebellar RNA but not from RNA isolated from Purkinje neurons (Fig. 7*A*). These results validated the relative absence of contamination by granule cells in the samples of isolated Purkinje neurons.

As shown previously (Richards et al. 2007), all four Ca$_v\beta$ variants were detected in whole cerebellum (Fig. 7*C*) and Purkinje neurons from WT mice (Fig. 7*B*). Similar results were obtained in extracts from total cerebellum of PV/CB$^{-/-}$ mice (Fig. 7*C*), but not in the extracts from single isolated Purkinje neurons of null-mutant mice (Fig. 7*B*). Ca$_v\beta_2$ was amplified from most (75%) WT Purkinje neurons and in a significantly smaller fraction (<50%, $P < 0.05$) of PV/CB$^{-/-}$ Purkinje neurons (Fig. 7*D*). Of the Ca$_v\beta_2$ splice variants expressed in mouse Purkinje neurons (β_{2a-d}), Ca$_v\beta_{2a}$ is the most prominent (Richards et al. 2007). Our results suggested that Ca$_v\beta_{2a}$ was specifically down-regulated in PV/CB$^{-/-}$ neurons below the threshold for detection in a one-step PCR protocol. We explored this possibility by quantitative PCR with Ca$_v\beta_{2a}$-specific primers (Supplemental Table S1). Because initial efforts to perform quantitative PCR with individual Purkinje neurons yielded inconsistent results, pools of 5–10 Purkinje neurons were analyzed with GAPDH as an internal reference. Consistent with the single-cell analyses, these experiments indicated levels of Ca$_v\beta_{2a}$ in PV/CB$^{-/-}$ neurons that were only 53 ± 8% of that in WT Purkinje neurons (Fig. 7*D*). The nearly twofold decrease in Ca$_v\beta_{2a}$ in PV/CB$^{-/-}$ neurons may therefore contribute to increased voltage-dependent inactivation of P-type currents in these neurons (Fig. 5*B*).

No differences in spontaneous firing properties in WT and PV/CB$^{-/-}$ neurons

Similar to their behavior in vivo, acutely isolated Purkinje neurons fire spontaneous APs that are driven primarily by voltage-gated Na^+ channels (Raman and Bean 1999). However, Ca$_v$2.1 channels can regulate this process through selective coupling to Ca^{2+}-activated (K_{Ca}) K^+ channels. By conducting Ca^{2+} signals that activate K_{Ca} channels, Ca$_v$2.1 channels control the afterhyperpolarization (AHP) and, subsequently, the spontaneous firing rate in Purkinje neurons (Edgerton and Reinhart 2003; Walter et al. 2006; Womack and Khodakhah 2002; Womack et al. 2004). To understand the physiological consequences of our findings, we asked whether increased voltage-dependent inactivation of P-type currents might affect spontaneous firing in PV/CB$^{-/-}$ Purkinje neurons.

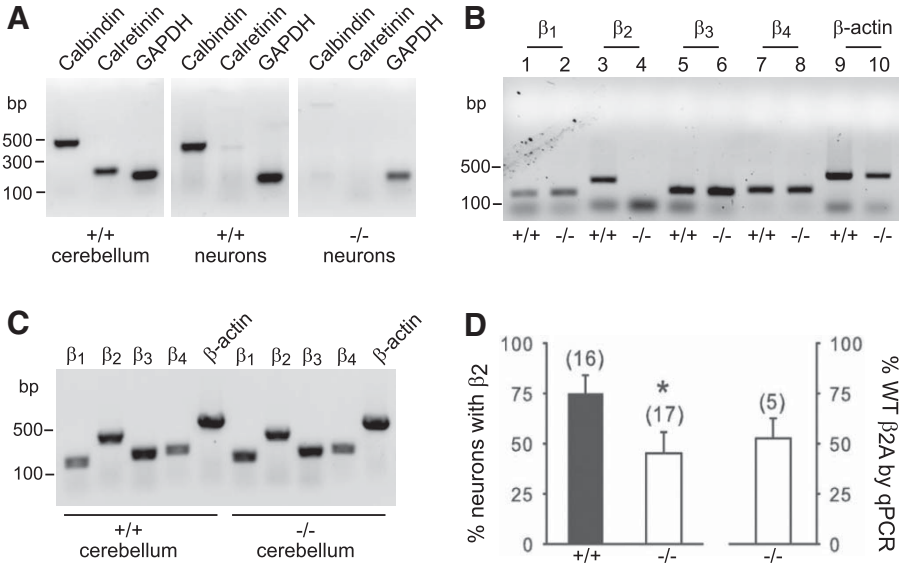

FIG. 7. Altered Ca$_v$2.1 subunit expression in PV/CB$^{-/-}$ Purkinje neurons. *A*: control experiment in which cerebellar tissue or pools of 5–10 Purkinje neurons from WT or PV/CB$^{-/-}$ mice were subjected to polymerase chain reaction (PCR) with primers specific for calbindin D-28k (*Calb1*, CB), calretinin (*Calb2*, CR), or GAPDH. *B*: representative experiment showing amplification of all 4 β subunits in WT Purkinje neurons ($n = 5$) and the absence of β_2 in PV/CB$^{-/-}$ neurons ($n = 5$). *C*: PCR analysis of Ca$_v\beta$ subunits (β_1–β_4) in cerebellar tissue from WT and PV/CB$^{-/-}$ mice. *D*: average results indicating percentage of individual neurons in WT and PV/CB$^{-/-}$ mice in which β_2 was detected (*left*). Parentheses indicate numbers of cells. $^{*}P < 0.05$ by *t*-test. *Right*: results from quantitative PCR from 5 to 10 Purkinje neurons using β_{2a}-specific primers. Relative levels of β_{2a} in WT and PV$^{-/-}$ neurons were determined as described in METHODS. Shown are averaged results from 5 independent experiments. GAPDH, glyceraldehyde-3-phosphate dehydrogenase.

At first glance, limited Ca^{2+} influx due to faster inactivation of $Ca_v2.1$ channels might inhibit K_{Ca} contribution to the AHP such that the spontaneous firing rate would be faster in PV/$CB^{-/-}$ neurons relative to that in WT. However, as endogenous Ca^{2+} buffers, PV and particularly the fast buffer CB could normally limit coupling between $Ca_v2.1$ Ca^{2+} signals and K_{Ca} channels. In this case, one would expect that in PV/$CB^{-/-}$ neurons, spontaneous firing might be slower than that in WT due to stronger K_{Ca}-mediated AHPs. On the other hand, the molecular switch to $Ca_v2.1$ channels that undergo stronger voltage-dependent inactivation in PV/$CB^{-/-}$ neurons might offset aberrant K_{Ca} activation, such that net excitability is unaltered. To test these possibilities, we compared spontaneous firing in isolated WT and PV/$CB^{-/-}$ Purkinje neurons in current-clamp recordings with physiological solutions at room temperature. Under these conditions, nearly all Purkinje neurons from WT and PV/$CB^{-/-}$ neurons fired spontaneously in the absence of injected current. There were no significant differences in AHP amplitude or other parameters of spontaneous APs in WT and PV/$CB^{-/-}$ neurons (Fig. 8, *A–F*). The mean interspike interval for WT and PV/$CB^{-/-}$ neurons was not significantly different (Fig. 8*G*), which indicated a similar firing rate in neurons from the two genotypes. We conclude that spontaneous firing of isolated Purkinje neurons is not perturbed in PV/$CB^{-/-}$ neurons, which may be due in part to compensatory functional changes in $Ca_v2.1$.

DISCUSSION

Our results reveal multiple mechanisms governing the behavior of P-type currents in Purkinje neurons. First, P-type currents undergo Ca^{2+}-dependent inactivation and facilitation, qualitatively similar to calmodulin-mediated regulation of recombinant $Ca_v2.1$ channels. Second, the inactivating profile of P-type currents during trains of AP stimuli may depend on the relative expression levels of different $Ca_v\beta$ subunits. Third, the Ca^{2+}-binding proteins PV and CB are required for maintaining the normal properties of the P-type current. Multifaceted regulation of $Ca_v2.1$ in Purkinje neurons may ensure the temporal precision of Ca^{2+} signals required for the control of motor coordination.

Ca^{2+}-dependent inactivation and facilitation of $Ca_v2.1$ in Purkinje neurons

Although the molecular details underlying $Ca_v2.1$ modulation by Ca^{2+}/calmodulin have been elucidated at the atomic level (Kim et al. 2008; Mori et al. 2008), the prevalence of Ca^{2+} feedback regulation of $Ca_v2.1$ in neurons is less clear. Ca^{2+}-dependent inactivation and facilitation were described for P-type currents in presynaptic terminals at the Calyx of Held (Cuttle et al. 1998; Forsythe et al. 1998) but were less robust for P/Q-type currents in chromaffin cells (Wykes et al. 2007). In rat Purkinje neurons, it was shown that P-type currents undergo Ca^{2+}-dependent facilitation, whereas Ca^{2+}-dependent inactivation was highly variable between cells (Chaudhuri et al. 2005). Ca^{2+}-dependent inactivation was measurable in most of the mouse Purkinje neurons in our study (Figs. 1*B* and 5), which may be due to a species- or age-related difference in $Ca_v2.1$ properties since we used older mice (14 to 21 days old) rather than young (6 to 10 days old) rats as in the previous study. Considering the net hyperpolarizing function of P-type Ca^{2+} currents through coupling to K_{Ca} channels (Edgerton and Reinhart 2003; Llinás and Sugimori 1980b; Raman and Bean 1999; Womack et al. 2004), Ca^{2+}-dependent inactivation of $Ca_v2.1$ may limit Ca^{2+} signals that would otherwise constrain the potential of Purkinje neurons to fire at high rates.

Our findings that Ca^{2+}-dependent facilitation of the P-type current in Purkinje neurons increases with spike frequency (Fig. 2*C*) are consistent with previous work in rat and mouse (Chaudhuri et al. 2005; Richards et al. 2007). Mechanistically, Ca^{2+}-dependent facilitation results from enhanced channel open probability due to Ca^{2+}-dependent conformational changes in calmodulin associated with $Ca_v2.1$ (Chaudhuri et al. 2007). This process may be intrinsically favored by repetitive depo-

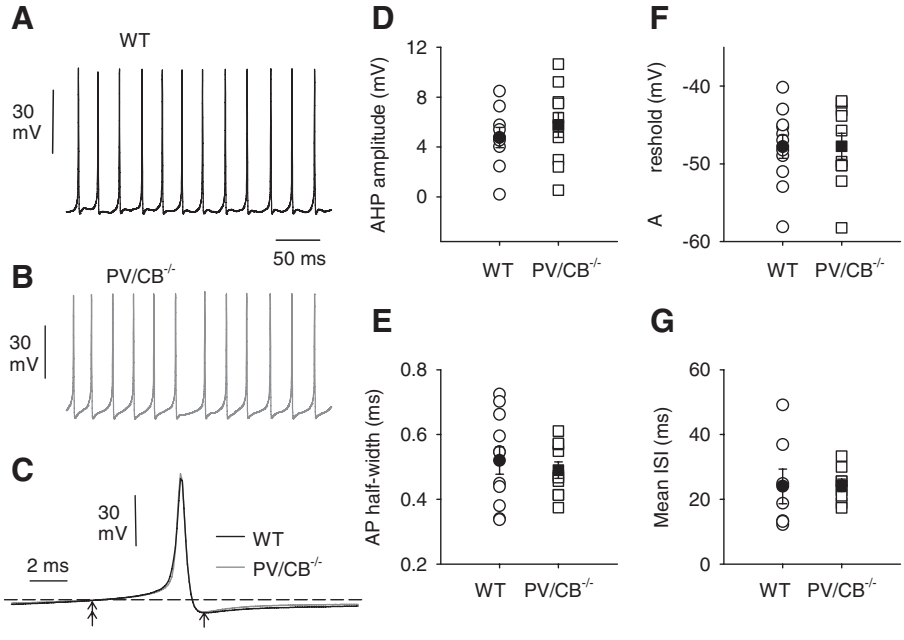

FIG. 8. No differences in spontaneous APs in WT and PV/$CB^{-/-}$ Purkinje neurons. Spontaneous APs were recorded from (*A*) WT and (*B*) PV/$CB^{-/-}$ neurons in current clamp without injected current. *C*: average AP waveform for WT (black trace, $n = 11$) and PV/$CB^{-/-}$ (gray trace, $n = 10$) neurons. For each neuron, averages are from all APs recorded in 10 consecutive sweeps of 500-ms duration. *D–G*: parameters for spontaneous APs in WT (circles) and PV/$CB^{-/-}$ (squares) neurons. Afterhyperpolarization (AHP) amplitude (*D*) was determined as the difference between the membrane potential measured 5 ms before the AP peak (double arrows in *C*) and the minimum membrane potential after the AP peak (single arrow in *C*). AP half-width (*E*) represents the duration of the AP at half-maximal amplitude from the threshold membrane potential. AP threshold (*F*) was measured at 5–15% of the tangential slope of the threshold depolarization. Mean interspike interval (ISI, *G*) is the average duration between peaks of the APs. Each symbol represents averaged data recorded as in *A* from one Purkinje neuron. Population averages are indicated with filled symbol (±SE).

larizations. Alternatively, high-frequency AP trains may somehow derepress Ca^{2+}-dependent facilitation of the P-type current. The presence of an endogenous inhibitor of Ca^{2+}-dependent facilitation was suggested from findings that intracellular perfusion of Purkinje neurons with recombinant calmodulin significantly increased Ca^{2+}-dependent facilitation of the P-type current (Chaudhuri et al. 2005). High-frequency stimulation may enhance the effectiveness of endogenous calmodulin in competing with this inhibitor, thus leading to greater Ca^{2+}-dependent facilitation for currents evoked by 200- than that by 100- and 50-Hz AP stimuli (Fig. 2*C*). In Purkinje neurons, increased recruitment of $Ca_v2.1$ by high-frequency stimulation may underlie activity-dependent Ca^{2+} signals required for $Ca_v2.1$ coupling to activation of calmodulin-dependent protein kinase (Mizutani et al. 2008) and depolarization-activated Ca^{2+} signals leading to long-term depression (Jin et al. 2007).

Altered $Ca_v2.1$ properties and Ca^{2+} homeostasis in PV/CB$^{-/-}$ Purkinje neurons

PV and CB act as mobile Ca^{2+} buffers, which can significantly alter the kinetics of Ca^{2+} signals in Purkinje neurons (Schmidt et al. 2003, 2007). We could not directly test whether PV and CB, like EGTA (Lee et al. 1999, 2000), might temper Ca^{2+}-dependent inactivation of the P-type current since the intrinsic properties of the P-type current differed in WT and PV/CB$^{-/-}$ Purkinje neurons (Figs. 5 and 6). Decreased contribution of $Ca_v\beta_{2A}$ subunits may permit greater voltage-dependent inactivation of P-type currents mediated by other $Ca_v\beta$ subunits in PV/CB$^{-/-}$ neurons (Fig. 7, *B* and *D*). However, this interpretation does not rule out the involvement of other mechanisms. Multiple $\alpha_1 2.1$ splice variants have been detected in Purkinje neurons (Bourinet et al. 1999). Some have variable cytoplasmic C-terminal domains (Kanumilli et al. 2006; Richards et al. 2007; Tsunemi et al. 2002), which can increase voltage-dependent inactivation of $Ca_v2.1$ (Krovetz et al. 2000). Increased expression of these variants could also contribute to the more strongly inactivating P-type currents in PV/CB$^{-/-}$ neurons.

Since PV and CB reach their mature expression levels in mice near P20 (Schwaller et al. 2002), it is tempting to speculate that increased $Ca_v2.1$ channel inactivation may be characteristic of the immature Purkinje neuron. Consistent with this possibility, in situ hybridization studies show that mRNA for $Ca_v\beta_2$ subunits is weak in P1 rat Purkinje neurons, but increase from P7 to P14 (Tanaka et al. 1995). Interestingly, $\alpha_1 2.1$ splice variants that undergo greater Ca^{2+}-dependent facilitation also increase in expression in rat Purkinje neurons during this age range (Chaudhuri et al. 2005). Developmental up-regulation of $Ca_v2.1$ subunits producing less inactivation and greater facilitation may increase the gain of Ca^{2+} signals because Ca^{2+} buffering strength increases due to the onset of PV and CB expression.

Although the spontaneous Purkinje cell firing properties were not different for WT and in PV/CB$^{-/-}$ mice in vitro (Fig. 8), the firing rate of single spikes from Purkinje neurons in vivo are higher in PV/CB$^{-/-}$ (~70 Hz) than that in WT mice (~45 Hz) (Servais et al. 2005). This difference may result from the influence of dendritic ion channels and synaptic inputs present in vivo that would not be retained in our in vitro recordings of dissociated Purkinje neurons. However, at the behavioral level, elimination of PV and CB results in only minor alterations in locomotor activity and coordination, not detectable in mice maintained under standard housing conditions (Bouilleret et al. 2000; Farre-Castany et al. 2007). In contrast to the severe ataxia exhibited by mice with loss-of-function mutations in the $Ca_v2.1$ α_1-subunit (Pietrobon 2005), the relatively modest motor phenotype in PV/CB$^{-/-}$ mice may result from recruitment of multiple homeostatic mechanisms. The volume of mitochondria—organelles with a high Ca^{2+} uptake capacity, yet rather slow Ca^{2+} uptake kinetics—is increased selectively in a subplasmalemmal zone in Purkinje cells deficient for PV (Chen et al. 2006). In addition, the volume and length of dendritic spines are increased in Purkinje neurons from mice lacking CB (Vecellio et al. 2000). Together with $Ca_v2.1$ channels undergoing greater inactivation, these morphological changes may help Purkinje neurons cope with activity-dependent increases in Ca^{2+} that might otherwise degrade their information-encoding potential.

Our results are the first to demonstrate alterations in $Ca_v2.1$ channels as a consequence of loss of PV and CB. In addition to Purkinje neurons, PV and CB are highly expressed in distinct populations of interneurons (Celio 1990), where their expression is reduced following seizure activity (Kim et al. 2006; Magloczky et al. 1997). Modification of $Ca_v2.1$ properties through molecular switching of $\alpha_1 2.1$ splice variants and β subunits may represent a general mechanism to protect neurons against aberrant Ca^{2+} signaling and pathological Ca^{2+} overloads.

ACKNOWLEDGMENTS

We thank Drs. T. Snutch and E. Perez-Reyes for cDNAs; T. Grieco and I. Raman for advice on Purkinje neuron dissociation; and Dr. Frank Gordon for advice on statistical analyses.

GRANTS

This work was supported by National Institutes of Health Grants R01-NS-044922 and R01-DC-009433 to A. Lee, F31-NS-04975 to L. Kreiner, and S11-NS-055883 to M. Benveniste; American Heart Association and Israel Binational Science Foundation grants to A. Lee; and Swiss National Science Foundation Grants 3100A0-100400/1 and 310000-113518/1 to B. Schwaller.

REFERENCES

Bouilleret V, Schwaller B, Schurmans S, Celio MR, Fritschy JM. Neurodegenerative and morphogenic changes in a mouse model of temporal lobe epilepsy do not depend on the expression of the calcium-binding proteins parvalbumin, calbindin, or calretinin. *Neuroscience* 97: 47–58, 2000.

Bourinet E, Soong TW, Sutton K, Slaymaker S, Mathews E, Monteil A, Zamponi GW, Nargeot J, Snutch TP. Splicing of alpha 1A subunit gene generates phenotypic variants of P- and Q-type calcium channels. *Nat Neurosci* 2: 407–415, 1999.

Brody DL, Patil PG, Mulle JG, Snutch TP, Yue DT. Bursts of action potential waveforms relieve G-protein inhibition of recombinant P/Q-type Ca^{2+} channels in HEK 293 cells. *J Physiol* 499: 637–644, 1997.

Castellano A, Wei X, Birnbaumer L, Perez-Reyes E. Cloning and expression of a neuronal calcium channel β subunit. *J Biol Chem* 268: 12359–12366, 1993.

Celio MR. Calbindin D-28k and parvalbumin in the rat nervous system. *Neuroscience* 35: 375–475, 1990.

Chaudhuri D, Alseikhan BA, Chang SY, Soong TW, Yue DT. Developmental activation of calmodulin-dependent facilitation of cerebellar P-type Ca^{2+} current. *J Neurosci* 25: 8282–8294, 2005.

Chaudhuri D, Issa JB, Yue DT. Elementary mechanisms producing facilitation of $Ca_v2.1$ (P/Q-type) channels. *J Gen Physiol* 129: 385–401, 2007.

Chen G, Racay P, Bichet S, Celio MR, Eggli P, Schwaller B. Deficiency in parvalbumin, but not in calbindin D-28k upregulates mitochondrial volume

and decreases smooth endoplasmic reticulum surface selectively in a peripheral, subplasmalemmal region in the soma of Purkinje cells. *Neuroscience* 142: 97–105, 2006.

Cuttle MF, Tsujimoto T, Forsythe ID, Takahashi T. Facilitation of the presynaptic calcium current at an auditory synapse in rat brainstem. *J Physiol* 512: 723–729, 1998.

DeMaria CD, Soong T, Alseikhan BA, Alvania RS, Yue DT. Calmodulin bifurcates the local Ca^{2+} signal that modulates P/Q-type Ca^{2+} channels. *Nature* 411: 484–489, 2001.

De Waard M, Campbell KP. Subunit regulation of the neuronal α_{1A} Ca^{2+} channel expressed in *Xenopus* oocytes. *J Physiol* 485: 619–634, 1995.

Donato R, Page KM, Koch D, Nieto-Rostro M, Foucault I, Davies A, Wilkinson T, Rees M, Edwards FA, Dolphin AC. The ducky(2J) mutation in Cacna2d2 results in reduced spontaneous Purkinje cell activity and altered gene expression. *J Neurosci* 26: 12576–12586, 2006.

Edgerton JR, Reinhart PH. Distinct contributions of small and large conductance Ca^{2+}-activated K^+ channels to rat Purkinje neuron function. *J Physiol* 548: 53–69, 2003.

Farre-Castany MA, Schwaller B, Gregory P, Barski J, Mariethoz C, Eriksson JL, Tetko IV, Wolfer D, Celio MR, Schmutz I, Albrecht U, Villa AE. Differences in locomotor behavior revealed in mice deficient for the calcium-binding proteins parvalbumin, calbindin D-28k or both. *Behav Brain Res* 178: 250–261, 2007.

Fierro L, DiPolo R, Llano I. Intracellular calcium clearance in Purkinje cell somata from rat cerebellar slices. *J Physiol* 510: 499–512, 1998.

Forsythe ID, Tsujimoto T, Barnes-Davies M, Cuttle MF, Takahashi T. Inactivation of presynaptic calcium current contributes to synaptic depression at a fast central synapse. *Neuron* 20: 797–807, 1998.

Ito M. *The Cerebellum and Neural Control*, edited by Ito M. New York: Raven, 1984.

Jin Y, Kim SJ, Kim J, Worley PF, Linden DJ. Long-term depression of mGluR1 signaling. *Neuron* 55: 277–287, 2007.

Jun K, Piedras-Renteria ES, Smith SM, Wheeler DB, Lee SB, Lee TG, Chin H, Adams ME, Scheller RH, Tsien RW, Shin H-S. Ablation of P/Q-type Ca^{2+} channel currents, altered synaptic transmission, and progressive ataxia in mice lacking the α_{1A}-subunit. *Proc Natl Acad Sci USA* 96: 15245–15250, 1999.

Kanumilli S, Tringham EW, Payne CE, Dupere JR, Venkateswarlu K, Usowicz MM. Alternative splicing generates a smaller assortment of $Ca_V2.1$ transcripts in cerebellar Purkinje cells than in the cerebellum. *Physiol Genomics* 24: 86–96, 2006.

Kim EY, Rumpf CH, Fujiwara Y, Cooley ES, Van Petegem F, Minor DL Jr. Structures of Ca_V2 Ca^{2+}/CaM-IQ domain complexes reveal binding modes that underlie calcium-dependent inactivation and facilitation. *Structure* 16: 1455–1467, 2008.

Kim JE, Kwak SE, Kim DS, Won MH, Kwon OS, Choi SY, Kang TC. Reduced calcium binding protein immunoreactivity induced by electroconvulsive shock indicates neuronal hyperactivity, not neuronal death or deactivation. *Neuroscience* 137: 317–326, 2006.

Kreiner L, Lee A. Endogenous and exogenous Ca^{2+} buffers differentially modulate Ca^{2+}-dependent inactivation of $Ca_V2.1$ Ca^{2+} channels. *J Biol Chem* 281: 4691–4698, 2006.

Krovetz HS, Helton TD, Crews AL, Horne WA. C-Terminal alternative splicing changes the gating properties of a human spinal cord calcium channel alpha 1A subunit. *J Neurosci* 20: 7564–7570, 2000.

Lee A, Scheuer T, Catterall WA. Ca^{2+}/calmodulin-dependent facilitation and inactivation of P/Q-type Ca^{2+} channels. *J Neurosci* 20: 6830–6838, 2000.

Lee A, Wong ST, Gallagher D, Li B, Storm DR, Scheuer T, Catterall WA. Ca^{2+}/calmodulin binds to and modulates P/Q-type calcium channels. *Nature* 399: 155–159, 1999.

Liang H, DeMaria CD, Erickson MG, Mori MX, Alseikhan B, Yue DT. Unified mechanisms of Ca^{2+} regulation across the Ca^{2+} channel family. *Neuron* 39: 951–960, 2003.

Livak KJ, Schmittgen TD. Analysis of relative gene expression data using real-time quantitative PCR and the $2(-\Delta\Delta C(T))$ method. *Methods* 25: 402–408, 2001.

Llinás R, Sugimori M. Electrophysiological properties of in vitro Purkinje cell dendrites in mammalian cerebellar slices. *J Physiol* 305: 197–213, 1980a.

Llinás R, Sugimori M. Electrophysiological properties of in vitro Purkinje cell somata in mammalian cerebellar slices. *J Physiol* 305: 171–195, 1980b.

Ludwig A, Flockerzi V, Hofmann F. Regional expression and cellular localization of the α_1 and β subunit of high voltage-activated calcium channels in rat brain. *J Neurosci* 17: 1339–1349, 1997.

Magloczky Z, Halasz P, Vajda J, Czirjak S, Freund TF. Loss of calbindin-D28K immunoreactivity from dentate granule cells in human temporal lobe epilepsy. *Neuroscience* 76: 377–385, 1997.

McDonough SI, Mintz IM, Bean BP. Alteration of P-type calcium channel gating by the spider toxin omega-Aga-IVA. *Biophys J* 72: 2117–2128, 1997.

Mintz IM, Venema VJ, Swiderek KM, Lee TD, Bean BP, Adams ME. P-type calcium channels blocked by the spider toxin omega-Aga-IVA. *Nature* 355: 827–829, 1992.

Mizutani A, Kuroda Y, Futatsugi A, Furuichi T, Mikoshiba K. Phosphorylation of Homer3 by calcium/calmodulin-dependent kinase II regulates a coupling state of its target molecules in Purkinje cells. *J Neurosci* 28: 5369–5382, 2008.

Mori MX, Vander Kooi CW, Leahy DJ, Yue DT. Crystal structure of the Ca_V2 IQ domain in complex with Ca^{2+}/calmodulin: high-resolution mechanistic implications for channel regulation by Ca^{2+}. *Structure* 16: 607–620, 2008.

Ovsepian SV, Friel DD. The leaner P/Q-type calcium channel mutation renders cerebellar Purkinje neurons hyper-excitable and eliminates Ca^{2+}-Na^+ spike bursts. *Eur J Neurosci* 27: 93–103, 2008.

Park D, Dunlap K. Dynamic regulation of calcium influx by G-proteins, action potential waveform, and neuronal firing frequency. *J Neurosci* 18: 6757–6766, 1998.

Perez-Reyes E, Castellano A, Kim HS, Bertrand P, Baggstrom E, Lacerda AE, Wei XY, Birnbaumer L. Cloning and expression of a cardiac/brain beta subunit of the L-type calcium channel. *J Biol Chem* 267: 1792–1797, 1992.

Pietrobon D. Function and dysfunction of synaptic calcium channels: insights from mouse models. *Curr Opin Neurobiol* 15: 257–265, 2005.

Raman IM, Bean BP. Ionic currents underlying spontaneous action potentials in isolated cerebellar Purkinje neurons. *J Neurosci* 19: 1664–1674, 1999.

Richards KS, Swensen AM, Lipscombe D, Bommert K. Novel CaV2.1 clone replicates many properties of Purkinje cell CaV2.1 current. *Eur J Neurosci* 26: 2950–2961, 2007.

Schmidt H, Brown EB, Schwaller B, Eilers J. Diffusional mobility of parvalbumin in spiny dendrites of cerebellar Purkinje neurons quantified by fluorescence recovery after photobleaching. *Biophys J* 84: 2599–2608, 2003.

Schmidt H, Kunerth S, Wilms C, Strotmann R, Eilers J. Spino-dendritic cross-talk in rodent Purkinje neurons mediated by endogenous Ca^{2+}-binding proteins. *J Physiol* 581: 619–629, 2007.

Schwaller B, Meyer M, Schiffmann S. "New" functions for "old" proteins: the role of the calcium-binding proteins calbindin D-28k, calretinin and parvalbumin, in cerebellar physiology. Studies with knockout mice. *Cerebellum* 1: 241–258, 2002.

Servais L, Bearzatto B, Schwaller B, Dumont M, De Saedeleer C, Dan B, Barski JJ, Schiffmann SN, Cheron G. Mono- and dual-frequency fast cerebellar oscillation in mice lacking parvalbumin and/or calbindin D-28k. *Eur J Neurosci* 22: 861–870, 2005.

Sidman RL, Green MC, Appel S. *Catalogue of the Neurological Mutants of Mice.* Cambridge, MA: Harvard Univ. Press, 1965.

Snell GD. Ducky, a new second chromosome mutation in the mouse. *J Hered* 46: 27–29, 1955.

Sokolov S, Weiss RG, Timin EN, Hering S. Modulation of slow inactivation in class A Ca^{2+} channels by beta-subunits. *J Physiol* 527: 445–454, 2000.

Soong TW, DeMaria CD, Alvania RS, Zweifel LS, Liang MC, Mittman S, Agnew WS, Yue DT. Systematic identification of splice variants in human P/Q-type channel $\alpha_1$2.1 subunits: implications for current density and Ca^{2+}-dependent inactivation. *J Neurosci* 22: 10142–10152, 2002.

Starr TVB, Prystay W, Snutch TP. Primary structure of a calcium channel that is highly expressed in the rat cerebellum. *Proc Natl Acad Sci USA* 88: 5621–5625, 1991.

Stea A, Tomlinson WJ, Soong TW, Bourinet E, Dubel SJ, Vincent SR, Snutch TP. The localization and functional properties of a rat brain α_{1A} calcium channel reflect similarities to neuronal Q- and P-type channels. *Proc Natl Acad Sci USA* 91: 10576–10580, 1994.

Tanaka O, Sakagami H, Kondo H. Localization of mRNAs of voltage-dependent Ca^{2+}-channels: four subtypes of α_1- and β-subunits in developing and mature rat brain. *Mol Brain Res* 30: 1–16, 1995.

Tank DW, Sugimori M, Connor JA, Llinás RR. Spatially resolved calcium dynamics of mammalian Purkinje cells in cerebellar slice. *Science* 242: 773–777, 1988.

Tsunemi T, Saegusa H, Ishikawa K, Nagayama S, Murakoshi T, Mizusawa H, Tanabe T. Novel $Ca_v2.1$ splice variants isolated from Purkinje cells do not generate P-type Ca^{2+} current. *J Biol Chem* 277: 7214–7221, 2002.

Usowicz MM, Sugimori M, Cherksey B, Llinás R. P-type calcium channels in the somata and dendrites of adult cerebellar Purkinje cells. *Neuron* 9: 1185–1199, 1992.

Vecellio M, Schwaller B, Meyer M, Hunziker W, Celio MR. Alterations in Purkinje cell spines of calbindin D-28k and parvalbumin knock-out mice. *Eur J Neurosci* 12: 945–954, 2000.

Walter JT, Alvina K, Womack MD, Chevez C, Khodakhah K. Decreases in the precision of Purkinje cell pacemaking cause cerebellar dysfunction and ataxia. *Nat Neurosci* 9: 389–397, 2006.

Westenbroek RE, Sakurai T, Elliott EM, Hell JW, Starr TV, Snutch TP, Catterall WA. Immunochemical identification and subcellular distribution of the α_{1A} subunits of brain calcium channels. *J Neurosci* 15: 6403–6418, 1995.

Womack MD, Chevez C, Khodakhah K. Calcium-activated potassium channels are selectively coupled to P/Q-type calcium channels in cerebellar Purkinje neurons. *J Neurosci* 24: 8818–8822, 2004.

Womack MD, Khodakhah K. Active contribution of dendrites to the tonic and trimodal patterns of activity in cerebellar Purkinje neurons. *J Neurosci* 22: 10603–10612, 2002.

Womack MD, Khodakhah K. Dendritic control of spontaneous bursting in cerebellar Purkinje cells. *J Neurosci* 24: 3511–3521, 2004.

Wykes RC, Bauer CS, Khan SU, Weiss JL, Seward EP. Differential regulation of endogenous N- and P/Q-type Ca^{2+} channel inactivation by Ca^{2+}/calmodulin impacts on their ability to support exocytosis in chromaffin cells. *J Neurosci* 27: 5236–5248, 2007.